arXiv:cond-mat/0302074v2 22 Oct 2003

Finite-temperature order-disorder phase transition in a cluster model of decagonal tilings

Michael Reichert[1, 2, *] and Franz Gähler[1]

[1] *Institut für Theoretische und Angewandte Physik, Universität Stuttgart, D-70550 Stuttgart, Germany*

[2] *Fachbereich Physik, Universität Konstanz, D-78457 Konstanz, Germany*

(Dated: February 2, 2008)

In a recent paper [*Cluster Model of Decagonal Tilings* (to be published in Phys. Rev. B)], we have introduced a cluster model for decagonal tilings in two dimensions. This model is now extended to three dimensions. Two-dimensional tilings are stacked on top of each other, with a suitable coupling between adjacent layers. An energy model with interactions leading to a perfect decagonal quasicrystal at low temperatures is studied by Monte Carlo simulations. An order parameter is defined, and its dependence on temperature and system size is investigated. Evidence for a finite-temperature order-disorder phase transition is presented. The critical exponents of this transition are determined by finite-size scaling.

PACS numbers: 61.44.Br, 64.60.Cn

I. INTRODUCTION

It is well known[1] that, in two dimensions (2D), perfect quasicrystalline order cannot be stable at positive temperature if the interactions have finite range. At positive temperature, a 2D quasicrystal is always in the random tiling phase without long-range order, the "transition" from the ordered to the disordered state being at $T = 0$. For three-dimensional (3D) quasicrystals, on the other hand, this order-disorder phase transition is expected to occur at positive temperature.[2]

The low-temperature state is also called the *locked* phase,[2] because its phason degrees of freedom are frozen (locked). The high-temperature state is accordingly called *unlocked* phase. Here, the thermal energy is sufficiently high to excite the phason degrees of freedom.

3D axial quasicrystals, in particular decagonal ones, can usually be regarded as periodic stackings of 2D layers, each of which is quasiperiodic. Geometrically, these layers can be described as decorations of quasiperiodic tilings like the Penrose tilings. Henley[2] has proposed to model axial quasicrystals as stackings of 2D tilings with a suitable coupling between adjacent layers, in addition to the coupling inside the 2D layers. Such layered tiling models built up from 2D Penrose tilings have been studied by Jeong and Steinhardt,[3] who indeed found a finite-temperature order-disorder phase transition.

In a recent paper[4] (hereafter referred to as Paper I), we have introduced a cluster model for 2D decagonal tilings. In the present article, we will now extend this model to 3D stackings. Our aim is to investigate an order-disorder phase transition, too, but this time in the framework of *cluster coverings*.

In Sec. II, we first give a brief summary of Paper I, explaining the important features of our cluster model. This includes the principle of cluster density maximization and the ordering of random structures to perfect ones by a coupling between overlapping clusters. In Sec. III, we extend this model to 3D by stacking the 2D layers on top of each other. An additional coupling between adjacent layers is introduced. For this 3D model we define in Sec. IV an order parameter to distinguish between the ordered quasicrystalline phase at low temperatures and the disordered random tiling phase at high temperatures. By means of this order parameter, the 3D system can then be investigated for a potential order-disorder phase transition, which is done in Sec. V using Monte Carlo (MC) simulations.

II. TWO-DIMENSIONAL CLUSTER MODEL (BRIEF SUMMARY)

In Paper I, different versions of overlap rules for clusters in a 2D covering model of the Penrose pentagon tiling (PPT) are discussed. The first version, which has a very natural realization in terms of a vertex cluster in the PPT (Fig. 1), is called the *relaxed* rule. If we compare this cluster with the well known Gummelt decagon,[5,6,7] we see that it enforces the correct orientation of the large B-overlaps, but not the orientation of the smaller A-overlaps (Fig. 1).

As an alternative to *cluster covering* as an ordering principle for quasicrystals, the principle of *cluster density maximization* is considered as well. A statistical model is built where each random tiling is assigned an energy

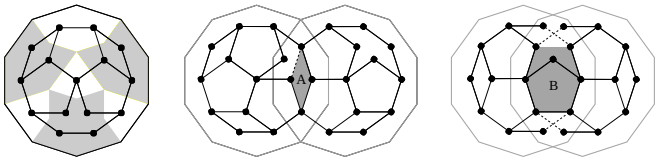

FIG. 1: Vertex cluster, superimposed on the Gummelt decagon (left), representative A-overlap (middle) and B-overlap (right). This cluster enforces the relaxed overlap rule.

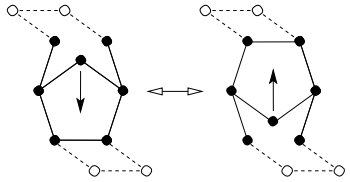

FIG. 2: Representative example of a flip move in the PPT. (The complete set of possible flip configurations is shown in Paper I.)

which is just the negative of the number of vertex clusters, thus mimicking the cohesion energy of the clusters.

The density of clusters can then be maximized in a MC simulation by simulated annealing, using flip moves like the one shown in Fig. 2. The simulation algorithm was a usual Metropolis importance sampling scheme:[8,9] A proposed flip is accepted with probability $p = 1$ if it decreases the energy ($\Delta E < 0$), but only with probability $p = \mathrm{e}^{-\beta \Delta E}$ if the energy is increased ($\Delta E > 0$).

The states of maximal cluster density are supertile random PPTs (Fig. 3) with an edge length τ^2 times that of the underlying tiling (where $\tau = (1+\sqrt{5})/2$ is the golden number). Naturally, they contain also cluster overlaps which do not satisfy the constraints of Gummelt's *perfect* overlap rule, since the *relaxed* rule does allow for disoriented A-overlaps because of the missing interior orientation of the rhombus (Fig. 1).

In a second step, a *coupling between overlapping clusters* is added which penalizes such defects. To keep the cluster density constant, the simulations are run at the level of the supertiling. Each cluster is represented by a vertex plus an arrow indicating the orientation of the cluster (Fig. 4).

As MC moves we can still use hexagon flips like the ones in Fig. 2, provided that the orientations of neighboring clusters are updated consistently with the underlying tiling (Fig. 5, left). Additionally, on the level of the supertiling there is a new type of flip: The rhombus flip (Fig. 5, right) only changes the orientations of the clusters on the obtuse rhombus corners, but keeps the tiling itself fixed. In comparison with the basic flip moves in the Penrose rhombus tiling[2,9] (which were used in the simulations of Jeong and Steinhardt[3]), the hexagon flip corresponds to D-type configurations and the rhombus flip to Q-type configurations of the Penrose rhombus tiling.[10]

As can be seen from Fig. 5, it is possible to create, annihilate, or shift defects by these flips. The defects correspond to tile edges with antiparallel arrows at their ends (marked in Fig. 5). Hence, we assign a positive energy to the creation of a new defect and use this energy model in a Metropolis MC scheme.

By simulated annealing it is shown that the cluster coupling model is capable of ordering the supertile random PPTs to perfectly quasiperiodic structures at low temperatures. Since, in our 3D simulations, we want to study transitions between perfect order and disorder, we will use this second kind of model for the layers in our

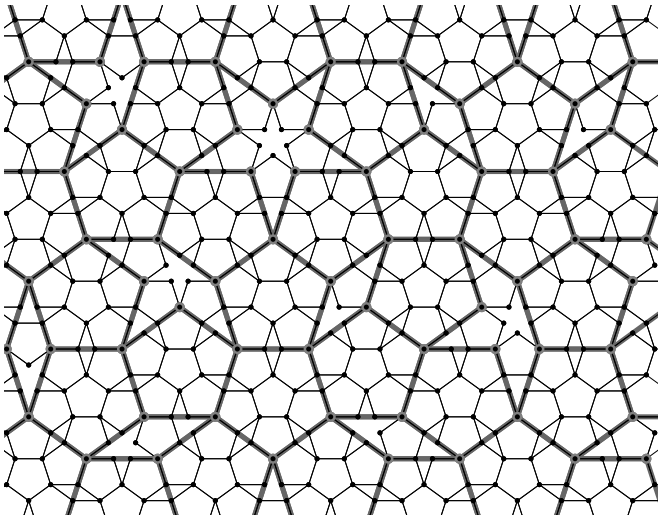

FIG. 3: Structure with maximal cluster density. The cluster centers form the vertices of a supertile random PPT (gray lines).

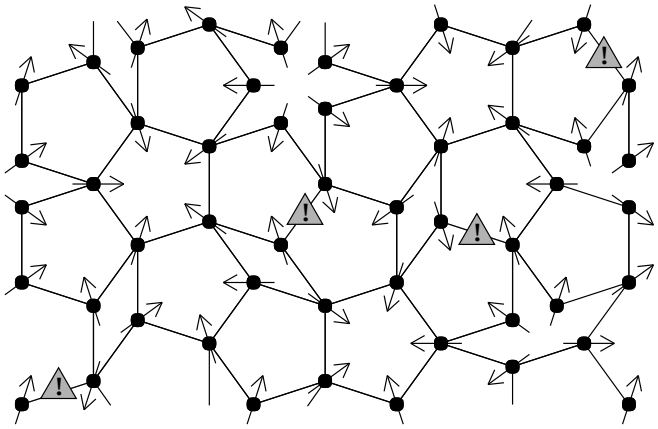

FIG. 4: Supertiling with cluster orientations indicated by arrows. The forbidden A-overlaps, corresponding to tile edges with antiparallel arrows, are marked.

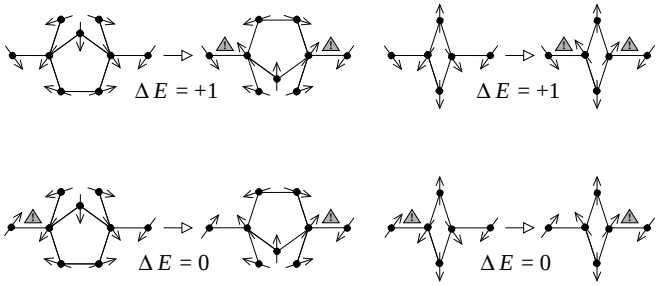

FIG. 5: Creation (top) and shift of defects (bottom) by single flips of the two types: hexagon flip (left) and rhombus flip (right).

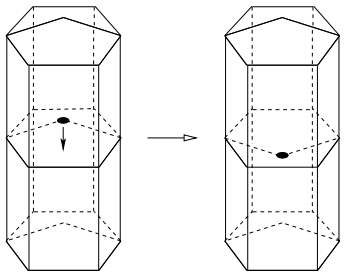

FIG. 6: Flip constraint for the interlayer coupling. The flip of the interior vertex of the middle-layer hexagon violates the congruence of the layers and hence costs energy.

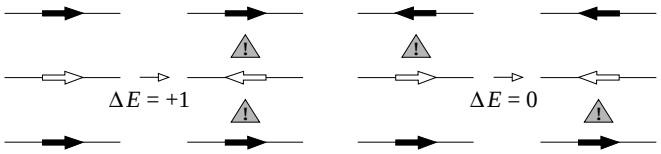

FIG. 7: Creation (left) and shift of interlayer defects (right). The arrows represent here schematically the orientations of hexagons or rhombi, respectively, in the layers.

stacking of coverings.

III. EXTENSION TO THREE DIMENSIONS

We will now consider 3D stackings of our 2D covering model. The *intra*layer interactions are those discussed above, which favor Gummelt's overlap rule, and hence produce perfectly ordered structures inside a layer at low temperatures. In addition, a new coupling *between* the layers has to be introduced. This *inter*layer coupling is chosen such that it prefers adjacent layers to be congruent. Then the ground state consists of identical, perfectly orderd layers. In the high-temperature state, the individual layers are random tilings which need not to be congruent, so that there is also disorder in the stacking direction.

Following an idea of Henley[2] and analogously to Jeong and Steinhardt,[3] we formulate a *flip constraint* for the *inter*layer coupling. The vertex inside a hexagon in a certain layer can be flipped only if there is also a hexagon with coinciding boundary (ignoring the interior vertex) in the adjacent layers above and below (Fig. 6). An analogous rule is imposed for rhombus flips: There must be a coinciding rhombus above and below in order that the middle rhombus can be flipped. These constraints maintain a minimal correlation between adjacent layers.

As we want to favor congruent layers in the ground state, energies are assigned to any mismatch between adjacent layers. A flip can then either create or remove two mismatches, or it can shift a mismatch up- or downwards (Fig. 7).

IV. DEFINITION OF AN ORDER PARAMETER

In order to analyse the transition from the disordered phase at high temperatures to the ordered phase at low temperatures, a suitable order parameter has to be defined, which can distinguish between perfect order and disorder.[3,11]

Within one layer, perfect order means the absence of disoriented A-overlaps, as discussed in Sec. II. In a continuous sequence of hexagons and rhombi along a straight line (Fig. 8), the orientations are then all the same, whereas a disoriented A-overlap switches to the opposite orientation. These lines correspond to the so called "worms" or "Ammann lines" in the Penrose rhombus tiling,[12,13] where again the rhombus in the PPT corresponds to Q-type configurations of Penrose rhombi, and the hexagon to D-type configurations. Flipping a hexagon or a rhombus in a perfect worm creates mismatches and interrupts the sequence of equal orientations along the worm line.

Therefore, if we characterize the orientation of each hexagon and rhombus along a straight line by a variable $s_i = \pm$ (Fig. 8), we can compare the worm line to a 1D "spin chain", assigning "spin up" for one orientation of hexagons and rhombi and "spin down" for the other. If we sum up all the spin variables s_i along a line, they will average out to zero in the random tiling phase. In the ordered phase, all the spins have the same orientation, so that the sum is proportional to the length of the chain.

We extend this picture to 3D by combining spin chains atop each other to "spin sheets" (Fig. 9), comparable to a 2D spin system. In the ordererd phase, all the layers are congruent, and thus all the spins within one sheet have the same orientation. In the disordered phase, the sum over all spins in a sheet will again be zero. However, even in the perfectly ordered phase, parallel spin sheets do not necessarily have the same spin orientations. Therefore, absolute values have to be taken for each sheet separately. The *order parameter* ("magnetization") thus becomes

$$M = \frac{1}{n} \sum_{\{\mathcal{S}_j\}} \left| \sum_{i \in \mathcal{S}_j} s_i \right| , \qquad (1)$$

where n is the number of spins (hexagons and rhombi) considered. The inner sum, of which the absolute value is taken, runs over all hexagons and rhombi (spins s_i)

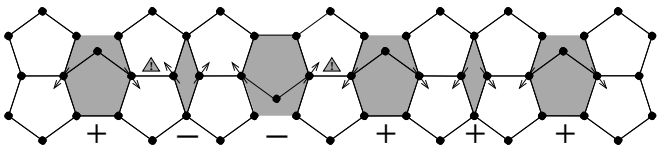

FIG. 8: Worm line consisting of hexagons and rhombi. Each hexagon and rhombus is assigned a "spin variable" + or −. The presence of defects leads to an alternation of the value of this variable along the line.

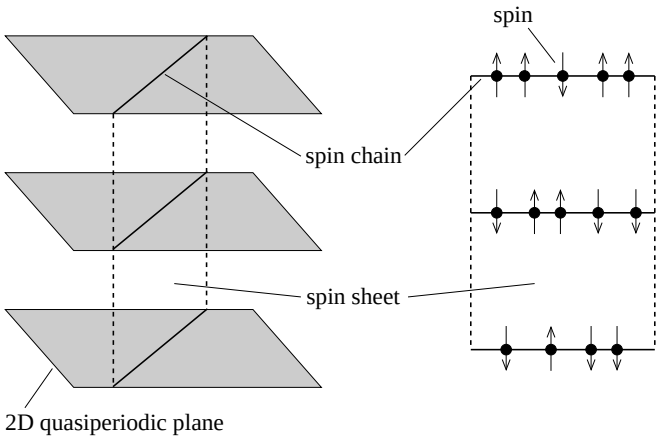

FIG. 9: "Spin chains" one atop the other are combined to a "spin sheet".

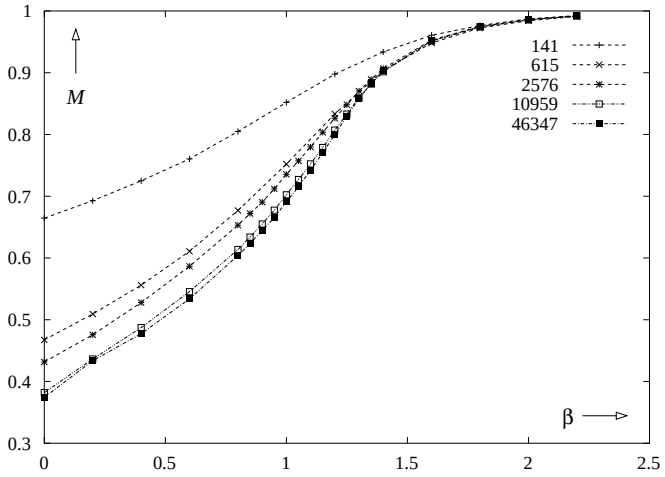

FIG. 10: System size dependence of the sheet magnetization vs. inverse temperature.

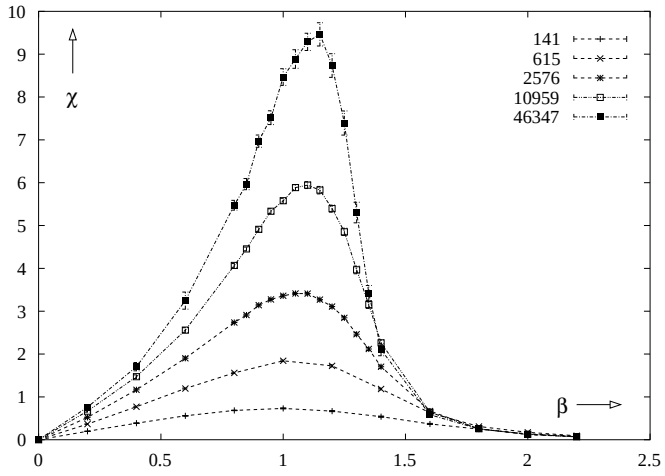

FIG. 11: System size dependence of the susceptibility vs. inverse temperature.

lying in the jth spin sheet $\mathcal{S}_j$. Afterwards, the contributions of all parallel spin sheets $\mathcal{S}_j$ are added. Such an order parameter is defined separately for each of the five directions in the tiling. As we have to use periodic approximants with periodic boundary conditions, some spin sheets may wrap around the torus several times, which has to be taken into account when determining the index of the spin sheet on which a given spin is located.

The value of this order parameter is one in the perfectly ordered case, since then all the spins in a sheet have the same orientation. In the totally disordered phase, the spins average out to zero already along the chains, so that the order parameter is zero. The magnetization M therefore provides a well defined and suitable order parameter for the detection of perfect quasiperiodic order.

In addition to the magnetization, we also define the corresponding "susceptibility" χ, which measures the *fluctuations* of the order parameter. In analogy to the magnetic susceptibility, we set

$$\chi = n\beta \left(\langle M^2 \rangle - \langle M \rangle^2 \right) , \qquad (2)$$

where β is the inverse temperature.

V. ORDER-DISORDER PHASE TRANSITION

The behavior of the order parameter has been investigated by MC simulations at different temperatures, using a series of stacked periodic approximants. In order to work out real 3D effects, the number of layers is proportional to the linear dimension of the approximant. We used approximants of order f_{k+1}/f_k in the x-direction, and of order f_k/f_{k-1} in the y-direction. which have the least number of defects.[14] f_k is the kth Fibonacci number ($f_0 = 0$, $f_1 = 1$, $f_{k+1} = f_k + f_{k-1}$). The linear dimension is then of the order of f_{k-1}, so that we took f_{k-1} layers in the stacking direction. This resulted in systems with total vertex numbers $N = 141$ ($k = 5$), 615 (6), 2576 (7), 10959 (8), and 46347 (9). The run lengths were of the order of some 100,000 MC sweeps at each temperature, where perfoming one MC sweep means to choose N-times a vertex randomly. The correlation time was found to be short compared to the run length, although no precise measurement has been made.

A Metropolis importance sampling scheme[3,8,9] is used for the simulations, similar to the one used in Paper I for the 2D simulations. For each proposed MC move, the total energy change ΔE due to intralayer *and* interlayer couplings is computed. The move is then accepted with probability $p = 1$ if the energy is decreased and with probability $p = \mathrm{e}^{-\beta \Delta E}$ if the energy is increased. The results for the magnetization and the susceptibility are shown in Figs. 10 and 11, respectively, for one representative direction in the tiling.

Fig. 10 illustrates how the magnetization curves converge to $M = 1$ at zero temperature ($\beta \to \infty$). Furthermore, the magnetization at a fixed temperature above the critical point ($\beta < \beta_c$, with $\beta_c \approx 1.2$) decreases with

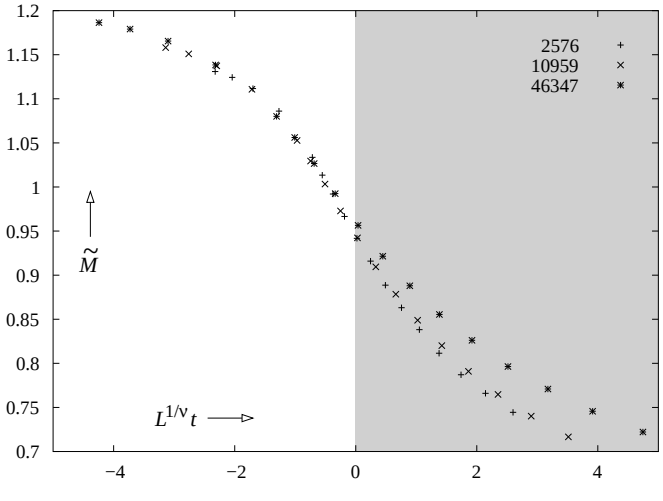

FIG. 12: Finite-size scaling plots $L^{\beta/\nu}M$ vs. $L^{1/\nu}t$ for the magnetization with the exponents $\beta = 0.08$ and $\nu = 1.6$. The critical exponent β and hence the scaling function $\tilde{M}$ are only defined below the critical temperature, i. e., for the data collapse only the range $t \leq 0$ has to be considered.

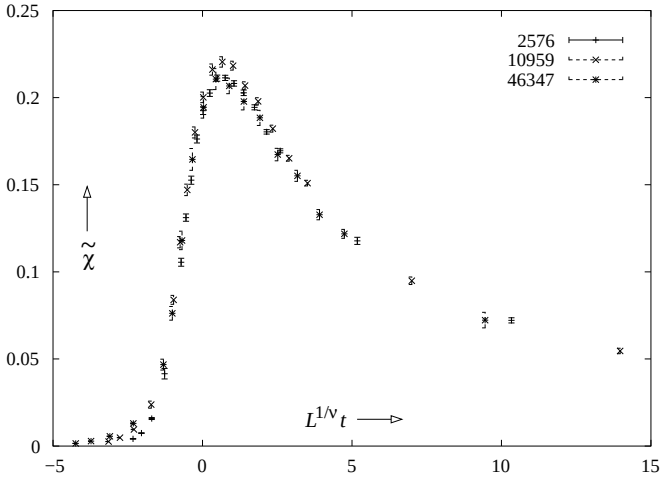

FIG. 13: Finite-size scaling plots $L^{-\gamma/\nu}\chi$ vs. $L^{1/\nu}t$ for the susceptibility with the exponents $\gamma = 1.7$ and $\nu = 1.6$.

increasing system size. The magnetization curves should tend to $M = 0$ at temperatures above the critical point, but they do so only very slowly. This can be understood as follows. In the random tiling phase, many spin sheets contain only very few spins, so that on those sheets the spins do not completely average out to zero. If for the magnetization only sheets are taken into account which contain a number of spins sufficiently high for a good statistics within the sheet, the value of M can be decreased considerably. At $\beta = 0$, M decreases for the system with 10959 vertices from $M \approx 0.4$ down to $M \approx 0.1$, and even further down to $M \approx 0.08$ for a larger system with about 75000 vertices.

The magnitude of the susceptibility, shown in Fig. 11, seems to diverge close to the transition temperature with increasing system size, which is another evidence for a phase transition. The maximum of the susceptibility yields a critical temperature of $\beta_c \approx 1.2$ in the limit of infinite system size.

Both the behavior of the magnetization and the susceptibiliy are consistent with a temperature-driven transition between the ordered (locked) and the disordered (unlocked) phase. To obtain the critical exponents of this phase transition, the method of finite-size scaling[8] has been used to fit the measured curves for magnetization $M_L(t)$ and susceptibility $\chi_L(t)$ to the scaling functions

$$\tilde{M}(L^{1/\nu}t) \;=\; L^{\beta/\nu}M_L(t) \quad (\text{for } t \leq 0)\,, \tag{3}$$

$$\tilde{\chi}(L^{1/\nu}t) \;=\; L^{-\gamma/\nu}\chi_L(t)\,, \tag{4}$$

where L is a characteristic length of the system (we use $L = N^{1/3}$) and $t = T/T_c - 1$ the reduced temperature (with $T_c = 1/\beta_c$). The critical exponents β and γ are defined by the behavior of magnetization and susceptiblity close to the transition temperature:

$$M \;\propto\; |T - T_c|^{\beta} \quad (\text{for } T \leq T_c)\,, \tag{5}$$

$$\chi \;\propto\; |T - T_c|^{-\gamma}\,. \tag{6}$$

The critical exponent ν, which determines the behavior of the correlation length, $\xi \propto |T - T_c|^{-\nu}$, has not been measured explicitly. By fitting the parameters β, γ, and ν in Eqs. (3) and (4) such that all the curves superimpose (Figs. 12 and 13), we obtain the critical exponents

$$\beta \;\approx\; 0.08\,, \tag{7}$$

$$\gamma \;\approx\; 1.7\,, \tag{8}$$

$$\nu \;\approx\; 1.6\,. \tag{9}$$

The uncertainty of these values is about 10% for γ and ν. In the case of β, the spread of values giving a reasonable fit is even larger.

We have also measured the energy E and the specific heat $C = N^{-1}\beta\left(\langle E^2\rangle - \langle E\rangle^2\right)$, where N is the number

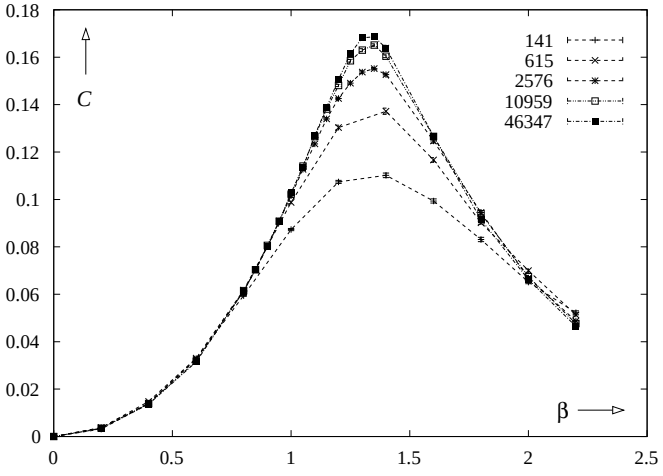

FIG. 14: System size dependence of the specific heat vs. inverse temperature.

of vertices and β the inverse temperature. The result is shown in Fig. 14. The maximum of the curve is close to the transition temperature determined above. It seems that the magnitude of the specific heat is independent of the system size (for large enough systems), which implies a critical exponent of $\alpha \approx 0$, where α is defined by $C \propto |T - T_c|^{-\alpha}$ close to the critical point. This is in agreement with the scaling relation $\alpha + 2\beta + \gamma = 2$ (Rushbrooke's law).[8]

For comparison, the values obtained by Jeong and Steinhardt[3] for stackings of Penrose rhombus tilings are $\beta = 0.2$, $\gamma = 1.6$, $\nu = 1.6$, and $\alpha = 0$. These values are in good agreement with our result (except for the exponent β, whose uncertainty is relatively large in our case).

VI. SOME FURTHER REMARKS

To test the reliability of our results, we have run simulations with different ratios of the intralayer and interlayer coupling strength. It is evident that this influences the value of the critical temperature and hence leads to different temperature scales. Normalizing the temperature to the particular critical point, i. e., using β/β_c as temperature scale, we obtain the same behavior of the magnetization, independent of the relative coupling strengths (Fig. 15). Only the curves where one of the coupling energies is set to zero show a different behavior, especially when the energy for the cluster coupling is zero, labeled by (0,1). In this case, there is no interaction inside the layers, so the order parameter is minimal, i. e., zero for infinite system size (see discussion of Fig. 10 in Sec. V). On the other hand, in the case (1,0) where the coupling energy in stacking direction is zero, there

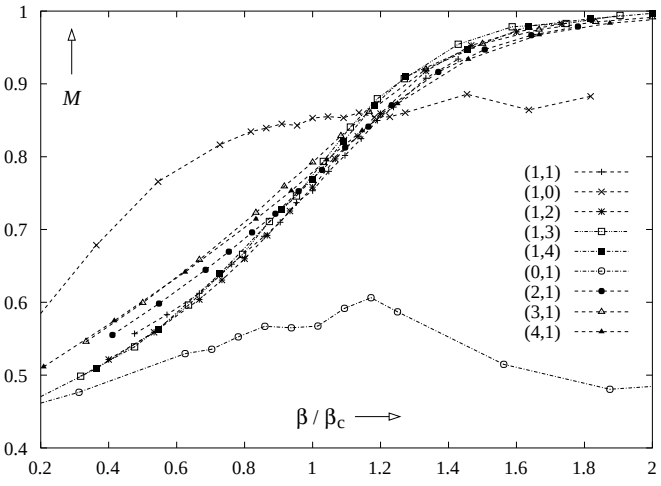

FIG. 15: Behaviour of the sheet magnetization for different ratios of intralayer and interlayer coupling strength. All curves are for the same approximant. The case of equal coupling strengths is labeled by (1,1), the case where the intralayer coupling is twice the interlayer coupling is labeled by (2,1), and so on.

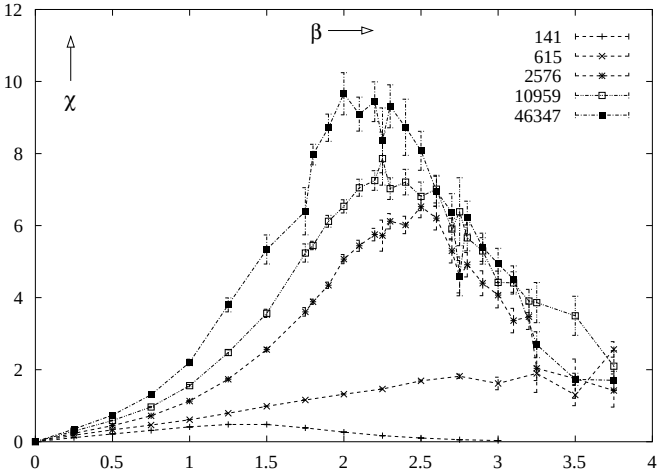

FIG. 16: System size dependence of the susceptibility vs. inverse temperature in the case of the relaxed rule.

is still some kind of purely geometrical coupling between the layers due to the flip constraint (Fig. 6). This yields an order parameter larger than zero. However, it does not approach $M = 1$ at high β (low temperatures) since this geometrical coupling only restricts the number of possible flips but does not enforce congruent layers.

We have also studied a 3D version of the *cluster density maximization* model obeying the *relaxed* rule (Sec. II). In this case, the intralayer energy is just the negative of the number of clusters. (For the interaction in stacking direction we keep the coupling described in Sec. III). Each ground state now consists of supertile random PPTs in each layer, which are all congruent. These supertile random PPTs are locally ordered, but show disorder at larger scales in terms of disoriented A-overlaps which violate the *perfect* overlap rule. The question is whether this partial, local order distinguishes the ground state sufficiently from the disordered high-temperature state, so that a phase transition between the two can take place. We cannot answer this question yet, because the curves obtained for the magnetization are too "noisy" (although the error bars are small), and the behavior of the susceptibility (Fig. 16) does not allow to decide whether or not it diverges at the "critical point", at least not for the accessible system sizes. It could well be that the dynamics is confined to subsets of the phase space which are separated by high energy barriers from other such subsets, thus breaking the ergodicity of the simulation.

VII. SUMMARY

We have presented a cluster model for 3D decagonal quasicrystals which shows a continuous phase transition at finite temperature from the ordered low-temperature state to the disordered high-temperature state. Using the sheet magnetization as order parameter and its associated susceptibility, the critical exponents of this transi-

TABLE I: Comparison of the critical exponents

	α	β	γ	ν
Cluster model	**0.0**	**0.08**	**1.7**	**1.6**
Tiling model[3]	0.0	0.2	1.6	1.6
2D Ising model[15]	0	0.125	1.75	1
3D Ising model[16]	0.11	0.33	1.24	0.63

tion have been determined. Within the statistical errors, these critical exponents are in good agreement with the values obtained by Jeong and Steinhardt[3] for stackings of Penrose rhombus tilings (for comparison, see Table I).

The notion of spin sheets suggests a certain resemblance of our model to the 2D Ising model. Indeed, there is some similarity also in the critical exponents (Table I). We have to point out, however, that there is an essential difference to the 2D Ising model. The interaction between the clusters inside the layers is rather different from the interaction between the layers in the stacking direction, i. e., the interactions in the system are highly anisotropic. Furthermore, in the Ising model only next-neighbor interactions are considered, whereas in our cluster model (and also in the Penrose tiling) the coupling between the clusters (or the coupling which arises from the matching rules in the Penrose tiling, respectively) are of longer range. Hence, it is not too surprising that the critical exponents of the 2D Ising model deviate from the ones obtained for our model (and those obtained by Jeong and Steinhardt[3]). Nevertheless, one can say that the critical exponents for the 3D decagonal quasicrystals resemble those of the 2D Ising model more than those of the 3D Ising model.

* Present address: Fachbereich Physik, Universität Konstanz, D-78457 Konstanz, Germany; Electronic address: michael.reichert@uni-konstanz.de

[1] P. A. Kalugin, JETP Lett. **49**, 467 (1989).

[2] C. L. Henley, in *Quasicrystals: The State of the Art*, edited by D. P. DiVincenzo and P. J. Steinhardt (World Scientific, Singapore, 1991), p. 429.

[3] H.-C. Jeong and P. J. Steinhardt, Phys. Rev. B **48**, 9394 (1993).

[4] M. Reichert and F. Gähler, *Cluster Model of Decagonal Tilings* (to be published in Phys. Rev. B).

[5] P. Gummelt, Geometriae Dedicata **62**, 1 (1996).

[6] P. Gummelt and C. Bandt, Mat. Sci. Eng. A **294-296**, 250 (2000).

[7] P. Gummelt, *Combination of Cluster Covering Approach and Random Tiling Model* (preprint, 2002).

[8] M. E. J. Newman and G. T. Barkema, *Monte Carlo Methods in Statistical Physics* (Oxford University Press, New York, 1999).

[9] L.-H. Tang and M. V. Jarić, Phys. Rev. B **41**, 4524 (1990).

[10] N. G. de Bruijn, Nederl. Akad. Wetensch. Proc. Ser. A **84**, 53 (1981).

[11] T. Dotera and P. J. Steinhardt, Phys. Rev. Lett. **72**, 1670 (1994).

[12] J. E. S. Socolar, T. C. Lubensky, and P. J. Steinhardt, Phys. Rev. B **34**, 3345 (1986).

[13] A. Pavlovitch, Y. Gefen, and M. Kléman, J. Phys. A: Math. Gen. **22**, 4347 (1989).

[14] O. Entin-Wohlman, M. Kléman, and A. Pavlovitch, J. Phys. France **49**, 587 (1988).

[15] L. Onsager, Phys. Rev. **65**, 117 (1944).

[16] A. M. Ferrenberg and D. P. Landau, Phys. Rev. B **44**, 5081 (1991).